

MULTI-USER MULTI-KEY IMAGE STEGANOGRAPHY WITH KEY ISOLATION

Tzu-Ti Wei, Yu-Han Tseng, Jun-Yi Lin, Yu-Chee Tseng, Jen-Jee Chen

PAIRLab, College of AI
National Yang Ming Chiao Tung University, Taiwan (R.O.C.)

ABSTRACT

Steganography conceals secret information within innocuous carriers while preserving visual fidelity and enabling reliable recovery. Recent unified networks operate normally under untriggered conditions but switch to hidden steganographic tasks when triggered. PUSNet follows this paradigm by performing image purification during normal operation and steganographic embedding when activated. However, it supports only a single user with one key pair, limiting its applicability in multi-user settings. We propose **PUSNet-MK**, a multi-key extension that enforces strict key isolation via a **mismatched-key isolation loss**, effectively preventing cross-key decoding when a wrong key is applied. This design preserves the intended steganographic behavior while addressing a critical security limitation of PUSNet. Extensive experiments demonstrate that PUSNet-MK produces high-quality stego images and accurate secret recovery, while preventing unintended information leakage.

Index Terms—Image steganography, multi-user systems, multi-key embedding, key isolation, secure information hiding

1. INTRODUCTION

Steganography conceals secret information within ordinary carriers while keeping the presence of hidden content imperceptible. Early methods rely on handcrafted embedding rules in the spatial or frequency domains [1, 2], which suffer from limited capacity and weak robustness, and are vulnerable to statistical steganalysis and common image perturbations. Recent deep learning approaches enable end-to-end optimization of hiding and recovery networks [3, 4, 5, 6, 7], learning adaptive embedding strategies that produce visually indistinguishable stego images with improved payload capacity and reliable secret extraction. Despite these advances, most deep steganography frameworks still operate with fixed embedding or decoding configurations, limiting their flexibility in security-critical scenarios.

Among recent advances, PUSNet [8] introduces a unified framework that integrates steganographic embedding, secret recovery, and purified image reconstruction via key-activated task switching. By using a predefined key pair, the network

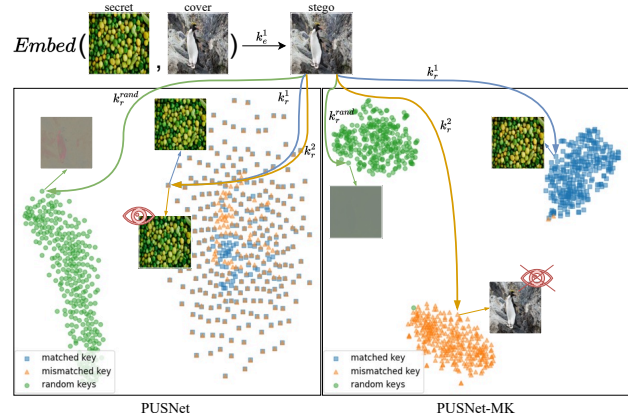


Fig. 1. PCA. Recovery features in PUSNet using matched and mismatched keys reveal feature entanglement. PUSNet-MK resolves this problem through key isolation.

is triggered to perform steganographic tasks under a shared architecture. While effective, PUSNet is restricted to a single key pair, forcing all users to share the same embedding and recovery configuration. This design lacks user-level isolation and allows any key holder to decode secrets embedded by others, posing a critical security risk in multi-user environments.

In practical deployments, steganographic systems are often shared by multiple users, each requiring independent and confidential communication channels. Formally, a multi-user steganography system must support distinct key pairs such that a secret embedded with one key can only be recovered using its corresponding key. Failure to satisfy this property results in *cross-key decoding*, where unauthorized users can partially or fully recover secrets not intended for them. However, most existing deep steganography frameworks do not explicitly enforce key isolation. Consequently, naively extending single-key models to multi-user settings introduces fundamental security vulnerabilities. As shown by the PCA visualization in Fig. 1, directly extending PUSNet to multiple key pairs results in entangled feature distributions during stego recovery, underscoring the need for explicit key-conditioned feature isolation to ensure secure multi-key steganography.

To address the cross-key decoding problem, we propose

PUSNet-MK, a multi-key extension of PUSNet that enables multiple users to share a single backbone while enforcing strict key isolation. PUSNet-MK explicitly suppresses key-induced latent interference, ensuring that only the matched key yields meaningful secret recovery. Our contributions are summarized as follows:

- We extend PUSNet to support multiple encoder–decoder key pairs within a unified backbone, enabling scalable and secure multi-user steganography.
- We introduce a *mismatched-key isolation mechanism* that suppresses cross-key decoding by explicitly driving recoveries under mismatched keys toward non-informative (cover-like) outputs.
- Extensive scalability experiments demonstrate that PUSNet-MK preserves stego imperceptibility and secret fidelity comparable to the single-key baseline, while substantially strengthening key isolation.

2. RELATED WORKS

2.1. Deep Learning-based Steganography

Early image steganography methods mainly relied on hand-crafted embedding strategies in the spatial or transform domain, such as least significant bit (LSB) substitution and frequency-domain techniques [2, 9, 10, 11]. Recent advances in deep learning have significantly improved image steganography by enabling data-driven embedding and recovery. Baluja [3] first introduced an end-to-end convolutional framework for hiding images within images. Subsequent works further enhance imperceptibility and robustness through task-specific architectural designs, including HiD-DeN [6], which jointly optimizes hiding and reveal networks under adversarial constraints, and UDH [12], which leverages residual learning for improved visual fidelity. More recently, HiNet [13] proposes a reversible architecture to improve reconstruction accuracy and stability. PUSNet [8] extends this line of research by integrating image purification, secret embedding, and recovery within a unified network via key-activated weight filling. However, existing deep steganographic methods typically assume a single shared key and do not explicitly address multi-user key isolation.

2.2. Multi-user and Multi-key Learning

Multi-user settings have been studied in various learning systems where multiple users share a common model while requiring isolated behaviors or access control. In such scenarios, a shared backbone is often adopted for efficiency, with user-specific conditions or parameters used to differentiate functionalities [14, 15]. However, existing designs mainly focus on improving scalability or parameter efficiency and do

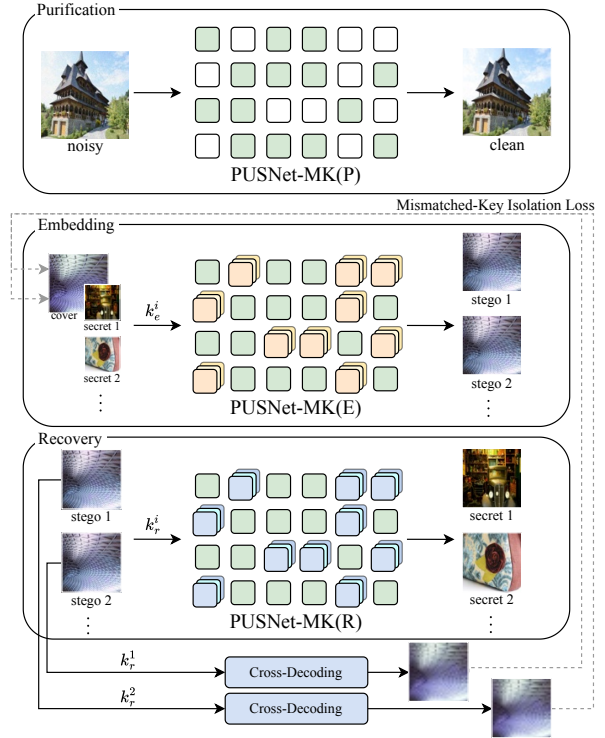


Fig. 2. PUSNet-MK framework. Green blocks are shared and learnable, while others are frozen and key-conditioned.

not explicitly address security concerns arising from user co-existence. Recent studies have shown that shared representations can lead to unintended information leakage across conditions or users when isolation is not carefully enforced [16]. In the context of steganography, this issue becomes particularly critical. However, strict key isolation in multi-user steganographic systems remains largely unexplored.

3. PROPOSED PUSNET-MK

PUSNet [8] introduces a unified formulation for image purification, secret embedding, and secret recovery using key-conditioned sparse weight filling within a single backbone. While effective in the single-key setting, this design does not generalize naturally to scenarios involving multiple independent keys. In particular, when multiple keys coexist under a shared backbone, mismatched but registered keys may still partially decode hidden content, resulting in cross-decoding and unintended information leakage. This observation indicates that the original PUSNet lacks strict key isolation and is therefore unsuitable for multi-key and multi-user deployments. In this section, we present PUSNet-MK, a multi-key extension that preserves the efficiency of the unified backbone while enforcing robust key isolation.

Table 1. Quantitative comparison. We report imperceptibility (I_{cover} vs. I_{stego}), recoverability (I_{secret} vs. $\tilde{I}_{\text{secret}}$), and cross decoding (I_{secret} vs. I_{secret}^*), where I_{secret}^* means a recovered secret using a wrong key.

Methods	DIV2K			COCO			ImageNet		
	PSNR \uparrow	SSIM \uparrow	MAE \downarrow	PSNR \uparrow	SSIM \uparrow	MAE \downarrow	PSNR \uparrow	SSIM \uparrow	MAE \downarrow
imperceptibility (I_{cover} vs. I_{stego})									
HiDDeN [4]	24.82/21.96	0.817/0.742	0.045/0.060	25.51/22.80	0.831/0.758	0.040/0.053	25.09/22.52	0.823/0.746	0.043/0.055
Baluja [3]	27.06/27.41	0.906/0.916	0.036/0.035	27.86/28.30	0.913/0.920	0.032/0.031	27.13/27.63	0.903/0.909	0.036/0.035
UDH [12]	30.18/31.35	0.887/0.901	0.024/0.021	30.56/31.93	0.879/0.893	0.023/0.020	30.35/31.68	0.871/0.886	0.024/0.020
HiNet [13]	32.04/31.66	0.866/0.865	0.020/0.021	32.91/32.63	0.865/0.864	0.017/0.018	32.81/32.54	0.862/0.861	0.018/0.018
PUSNet [8]	38.07/38.04	0.969/0.970	0.009/0.009	38.74/38.74	0.967/0.968	0.009/0.009	38.35/38.37	0.962/0.962	0.009/0.009
PUSNet-MK	33.77/33.65	0.959/0.957	0.017/0.017	34.47/34.40	0.959/0.958	0.015/0.015	34.05/33.93	0.951/0.950	0.016/0.016
recoverability (I_{secret} vs. $\tilde{I}_{\text{secret}}$)									
HiDDeN [4]	19.68/21.92	0.772/0.738	0.081/0.063	19.89/22.52	0.777/0.737	0.080/0.056	19.88/22.15	0.760/0.725	0.081/0.059
Baluja [3]	28.03/27.89	0.909/0.904	0.031/0.032	28.92/28.80	0.913/0.908	0.027/0.028	28.14/28.05	0.902/0.898	0.031/0.032
UDH [12]	22.83/26.38	0.826/0.872	0.062/0.039	23.03/26.92	0.833/0.860	0.060/0.036	23.02/26.83	0.821/0.855	0.061/0.037
HiNet [13]	25.88/25.75	0.826/0.840	0.040/0.041	26.31/26.02	0.815/0.825	0.038/0.040	26.11/25.90	0.808/0.819	0.039/0.041
PUSNet [8]	29.20/29.23	0.947/0.948	0.028/0.028	29.46/29.34	0.947/0.947	0.027/0.028	29.24/29.09	0.942/0.942	0.027/0.028
PUSNet-MK	32.21/31.83	0.949/0.948	0.019/0.020	33.17/32.79	0.952/0.951	0.017/0.018	32.64/32.28	0.946/0.943	0.018/0.019
cross decoding (I_{secret} vs. I_{secret}^*)									
HiDDeN [4]	19.21/20.67	0.740/0.730	0.092/0.071	19.07/21.18	0.740/0.730	0.094/0.064	19.03/20.89	0.720/0.720	0.094/0.067
Baluja [3]	19.21/20.00	0.771/0.792	0.086/0.080	19.06/19.70	0.774/0.788	0.086/0.082	18.88/19.43	0.764/0.779	0.089/0.085
UDH [12]	25.46/22.30	0.880/0.830	0.043/0.065	25.53/22.36	0.870/0.830	0.043/0.065	25.70/22.42	0.870/0.820	0.042/0.065
HiNet [13]	25.88/18.00	0.830/0.430	0.040/0.102	26.31/18.06	0.820/0.380	0.038/0.102	26.11/18.00	0.810/0.380	0.039/0.102
PUSNet [8]	29.53/28.36	0.945/0.943	0.026/0.031	29.81/28.55	0.945/0.942	0.026/0.030	29.43/28.46	0.940/0.938	0.027/0.030
PUSNet-MK	8.67/8.77	0.153/0.161	0.312/0.303	8.51/8.52	0.215/0.214	0.315/0.315	8.48/8.50	0.207/0.208	0.318/0.318

3.1. Review of PUSNet

Fig. 2 illustrates the PUSNet-MK framework. When only a single key pair is used, it is equivalent to PUSNet. PUSNet supports image purification (**P**), secret embedding (**E**), and secret recovery (**R**) by activating different subsets of network parameters via a sparse weight filling mechanism.

PUSNet first initializes a backbone weight set W and samples a random binary mask M according to a predefined sparse ratio α . The masked weights $W \odot M$ form a shared backbone across all tasks, while the complementary region $W \odot \bar{M}$ is reserved for task-specific adaptations. This design enables multiple functionalities to be realized within a single network without additional task-specific modules.

For image purification, the purified network operates as

$$N[W \odot M + W \odot \bar{M}](I_{\text{noisy}}) \rightarrow \tilde{I}_{\text{clean}}, \quad (1)$$

where I_{noisy} is derived from a clean image I_{clean} by adding Gaussian noise. During training, the optimization is restricted to the shared subset $W \odot M$ and the complementary subset $W \odot \bar{M}$ is frozen and excluded from parameter updates.

For steganographic embedding and recovery, PUSNet employs key-conditioned weight instantiation. Given a pair of keys (k_e, k_r) , a weight set W_e is generated by seed k_e and another W_r is generated by seed k_r via weights initialization method [17]. Weights W_e and W_r populate the complementary region \bar{M} to perform secret embedding and recovering tasks:

$$\begin{aligned} N[W \odot M + W_e \odot \bar{M}](I_{\text{secret}}, I_{\text{cover}}) &\rightarrow I_{\text{stego}} \\ N[W \odot M + W_r \odot \bar{M}](I_{\text{stego}}) &\rightarrow \tilde{I}_{\text{secret}} \end{aligned} \quad (2)$$

where I_{secret} and I_{cover} denote the secret and cover images, respectively. I_{stego} is the stego image obtained by embedding I_{secret} into I_{cover} , which is expected to be visually indistinguishable from I_{cover} . After recovery, the reconstructed secret $\tilde{I}_{\text{secret}}$ should be visually similar to I_{secret} . Again, during training, only the shared subset $W \odot M$ is optimized.

3.2. Multi-key Extension and Training Objectives

To support multiple key pairs, we preserve the original PUSNet architecture and extend it to the multi-key setting by enforcing strong key-conditioned separation in the recovery feature space as shown in Fig. 2. The subnetwork $W \odot M$ remains fully shared and jointly optimized across all normal and steganographic tasks, while each key pair activates its own embedding and recovery functions via its corresponding complementary subnetworks. This design enables multiple users to coexist within a unified backbone.

In the multi-key setting, PUSNet-MK allows K key pairs $\{(k_e^i, k_r^i)\}_{i=1}^K$. For each pair (k_e^i, k_r^i) , similar weight sets W_e^i and W_r^i are generated using keys as seeds. The secret embedding and recovering tasks are performed by:

$$\begin{aligned} N[W \odot M + W_e^i \odot \bar{M}](I_{\text{secret}}^i, I_{\text{cover}}^i) &\rightarrow I_{\text{stego}}^i \\ N[W \odot M + W_r^i \odot \bar{M}](I_{\text{stego}}^i) &\rightarrow \tilde{I}_{\text{secret}}^i \end{aligned} \quad (3)$$

The training remains the same—only the shared subset $W \odot M$ is optimized.

Cross-Key Decoding Problem. As shown in Eq. 3, all key pairs operate on the same shared backbone (i.e., M),

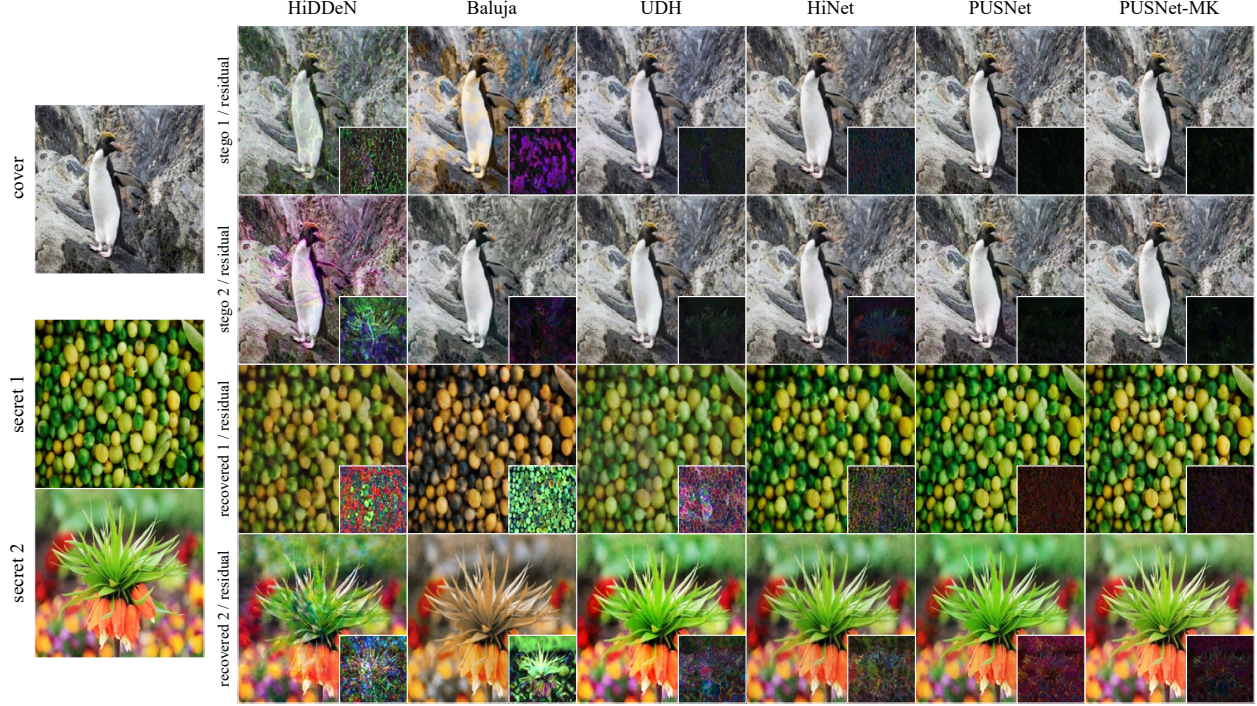


Fig. 3. Qualitative comparison. Stego and recovered images, with residuals shown in the lower-right corner.

while realizing distinct functionalities through their complementary regions (i.e., \bar{M}). Although this design enables unification within a single network, it also introduces the risk of *key interference*, where a mismatched key can partially recover recognizable secret content, thereby violating the security requirement of multi-user steganography. As illustrated in Fig. 1, we embed a secret using one key and attempt recovery with multiple keys. Without explicit key separation, the recovery features corresponding to matched and mismatched keys exhibit significant overlap, leading to unintended cross-key decoding and secret leakage. To meet the security requirements of multi-user steganography, we next present a solution that enforces strict separation among key-conditioned representations.

3.3. Training Objective and Key Separation

Following PUSNet, we jointly optimize the normal, steganographic embedding, and secret recovery tasks across all key pairs. In addition, we introduce a mismatched-key isolation loss to explicitly enforce strict key separation. The overall training objective promotes imperceptible stego generation, faithful secret recovery under matched keys, preserved purification capability, and non-informative outputs when mismatched keys are used.

Steganographic Losses. For each key pair (k_e^i, k_r^i) , $i = 1..K$, the secret embedding and recovery results are

optimized by:

$$\begin{aligned} \mathcal{L}_{\text{emb}} &= \sum_{i=1..K} \|I_{\text{stego}}^i - I_{\text{cover}}^i\|^2 \\ \mathcal{L}_{\text{rec}} &= \sum_{i=1..K} \|\tilde{I}_{\text{secret}}^i - I_{\text{secret}}^i\|^2. \end{aligned} \quad (4)$$

Purification Loss. To preserve the purification capability, the normal network is optimized by :

$$\mathcal{L}_{\text{pur}} = \|I_{\text{clean}} - \tilde{I}_{\text{clean}}\|^2. \quad (5)$$

Mismatched-Key Isolation Loss. To suppress cross-key decoding, a stego image produced by a key pair (k_e^i, k_r^i) but recovered by a mismatched key (k_e^j, k_r^j) , $i \neq j$, is forced to regress toward the cover image I_{cover} :

$$\mathcal{L}_{\text{mki}} = \sum_{i \neq j} \|N[W \odot M + W_r^j \odot \bar{M}](I_{\text{stego}}^i) - I_{\text{cover}}\|^2. \quad (6)$$

Total Loss. The final objective is to optimize:

$$\mathcal{L}_{\text{total}} = \lambda_e \mathcal{L}_{\text{emb}} + \lambda_r \mathcal{L}_{\text{rec}} + \lambda_p \mathcal{L}_{\text{pur}} + \lambda_m \mathcal{L}_{\text{mki}}. \quad (7)$$

$\mathcal{L}_{\text{total}}$ is used to train the shared weights in M . For each component in Eq. 7, the corresponding complementary weights in \bar{M} should be instantiated accordingly.

4. EXPERIMENTS

All models are trained on DIV2K [18] with images resized to 256×256 for 500 epochs using a single NVIDIA L40S

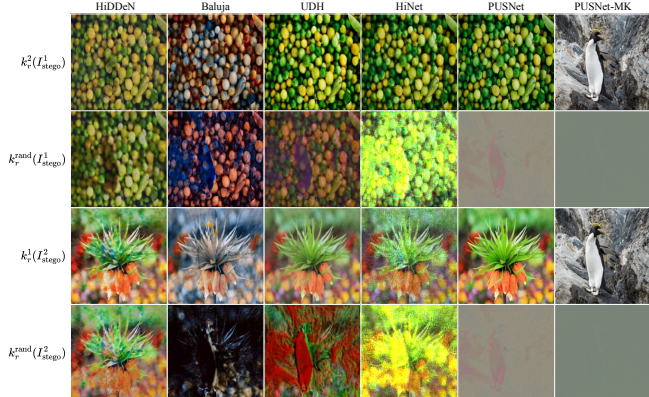


Fig. 4. Cross-key decoding tests. $k_r^j(I_{stego}^i) = N[W \odot M + W_r^j \odot \overline{M}](I_{stego}^i)$ denotes decoding I_{stego}^i with a mismatched key k_r^j , $i \neq j$, where *rand* means a random key.

GPU. We evaluate sparse ratios in the range $\alpha \in [0.5, 0.9]$. The original PUSNet with a direct multi-key extension serves as the primary baseline. Evaluation is conducted on DIV2K, COCO [19], and ImageNet [20], with all images resized to 512×512 . The hyperparameters are set to $\lambda_e = 1.0$, $\lambda_r = 0.75$, $\lambda_p = 0.25$, and $\lambda_m = 0.5$.

Quantitative Comparison. Table 1 reports quantitative results on *imperceptibility* (hiding quality), *recoverability* (secret fidelity), and *cross-key decoding* (leakage under mismatched keys), evaluated using PSNR, SSIM, and MAE. PUSNet-MK outperforms all competing methods in terms of recoverability and achieves substantially lower leakage in cross-key decoding with large margins. While the original PUSNet attains the best imperceptibility due to the absence of constraints on the recovery feature space, PUSNet-MK remains highly competitive, particularly in SSIM and MAE. These results confirm that PUSNet-MK effectively supports secure multi-key image steganography.

Qualitative Comparison. Fig. 3 presents qualitative comparisons under matched key settings. Most recent methods generate visually imperceptible stego images. As evidenced by the residual images, PUSNet-MK reconstructs secrets with the highest visual fidelity while maintaining competitive imperceptibility.

Cross-Key Decoding Test. Using the scenarios in Fig. 3, Fig. 4 presents cross-key decoding results. Most baselines recover noticeable secret structures under either mismatched or random keys, indicating insufficient key isolation. PUSNet reveals noticeable RGB information when a mismatched registered key is used and leaks minor structural information under a random key. In contrast, PUSNet-MK produces non-informative outputs under random keys and cover-like outputs under mismatched keys. These results demonstrate that PUSNet-MK effectively enforces strict key-conditioned separation and prevents unintended secret leakage.

	stego	2 keys		3 keys			4 keys			
0.9	key	33.14 0.951	8.95 0.124	25.33 0.916	9.02 0.124	8.86 0.121	29.47 0.928	9.03 0.126	8.86 0.122	8.78 0.120
		8.86 0.120	33.09 0.950	8.94 0.121	25.41 0.916	8.86 0.120	8.94 0.122	29.31 0.927	8.86 0.122	8.78 0.120
		8.86 0.120	33.09 0.950	8.94 0.122	9.02 0.125	25.09 0.911	8.94 0.123	9.03 0.127	29.16 0.926	8.78 0.120
0.7	key	33.22 0.951	8.94 0.124	28.91 0.924	9.04 0.127	8.88 0.123	20.19 0.862	9.03 0.125	8.86 0.124	8.77 0.120
		8.85 0.120	33.12 0.951	8.95 0.123	28.99 0.924	8.87 0.121	8.95 0.122	20.04 0.858	8.86 0.121	8.79 0.123
		8.85 0.120	33.12 0.951	8.95 0.126	9.03 0.125	28.98 0.925	8.96 0.125	9.02 0.125	20.13 0.860	8.77 0.120
0.5	key	29.72 0.924	8.96 0.126	26.50 0.903	9.01 0.121	8.84 0.121	23.92 0.846	9.09 0.133	8.90 0.123	8.82 0.121
		8.88 0.120	28.90 0.906	8.92 0.119	21.29 0.859	8.84 0.122	9.02 0.126	21.93 0.835	8.89 0.118	8.80 0.120
		8.88 0.120	28.90 0.906	8.92 0.120	9.02 0.125	23.85 0.887	9.02 0.126	9.10 0.127	24.3 0.846	8.83 0.126
						8.98 0.122	9.08 0.128	8.91 0.130	22.13 0.835	

Fig. 5. Scalability study. We vary the number of keys (K) and sparse ratio (α). Each confusion matrix shows recoverability, where rows correspond to stego images encoded with different keys and columns correspond to keys used for decoding. In each cell, we report PSNR (black) and SSIM (brown).

Scalability (K, α). Fig. 5 investigate the scalability of PUSNet-MK in terms of recoverability by varying K and ratio α . Across different α , matched-key decoding consistently achieves high reconstruction quality, as reflected by the strong diagonal responses. In contrast, cross-key decoding remains uniformly suppressed, with off-diagonal entries staying at a low level regardless of the number of keys. These results demonstrate its robustness and scalability for multi-user steganography.

5. CONCLUSIONS

We identify cross-key decoding as a key limitation of single-key steganographic frameworks in multi-user settings. To address this issue, we propose PUSNet-MK, a multi-key extension that allows multiple users to share a single backbone while enforcing strict key isolation. Experiments on three public datasets show that PUSNet-MK preserves steganographic imperceptibility and matched-key recovery performance, while effectively suppressing cross-key decoding. These results demonstrate the practicality of PUSNet-MK for secure and scalable multi-user steganography. Future work will explore extending the framework to alternative backbone architectures beyond CNNs.

6. REFERENCES

- [1] Jessica Fridrich, Miroslav Goljan, and Rui Du, “Reliable detection of lsb steganography in color and grayscale images,” *Proceedings of the 2001 Workshop on Multimedia and Security*, pp. 27–30, 2001.
- [2] Ingemar J. Cox, Matthew L. Miller, Jeffrey A. Bloom, Jessica Fridrich, and Ton Kalker, *Digital Watermarking and Steganography*, Morgan Kaufmann, 2nd edition, 2007.
- [3] Shumeet Baluja, “Hiding images in plain sight: Deep steganography,” in *Advances in Neural Information Processing Systems (NeurIPS)*, 2017, pp. 2068–2077.
- [4] Jiren Zhu, Russell Kaplan, Justin Johnson, and Fei-Fei Li, “Hidden: Hiding data with deep networks,” *arXiv preprint arXiv:1807.09937*, 2018.
- [5] Shumei Wu, Haichao Shi, Jian Dong, Zhihua Su, and Hui Xue, “Steganogan: High capacity image steganography with gans,” in *Proceedings of the IEEE/CVF Conference on Computer Vision and Pattern Recognition Workshops (CVPRW)*. IEEE, 2018, pp. 1682–1685.
- [6] Jamie Hayes and George Danezis, “Generating steganographic images via adversarial training,” *arXiv preprint arXiv:1703.00371*, 2017.
- [7] Ruoyu Zhang, Shunquan Dong, Jun Liu, and Yi Wang, “Advsteg: Adversarial steganography via generative adversarial networks,” *IEEE Access*, vol. 7, pp. 110038–110047, 2019.
- [8] Guobiao Li, Sheng Li, Zicong Luo, Zhenxing Qian, and Xinpeng Zhang, “Purified and unified steganographic network,” in *Proceedings of the IEEE/CVF Conference on Computer Vision and Pattern Recognition (CVPR)*, 2024, pp. 27569–27578.
- [9] Jessica Fridrich, *Steganography in digital media: principles, algorithms, and applications*, Cambridge university press, 2009.
- [10] Yu-Chee Tseng, Yu-Yuan Chen, and Hsiang-Kuang Pan, “A secure data hiding scheme for binary images,” *IEEE Transactions on Communications*, vol. 50, no. 8, pp. 1227–1231, 2002.
- [11] Yu-Chee Tseng and Hsiang-Kuang Pan, “Data hiding in 2-color images,” *IEEE Transactions on Computers*, vol. 51, no. 7, pp. 873–880, 2002.
- [12] Rui Zhang, Xia Dong, and Xinpeng Zhang, “Universal deep hiding for steganography,” in *Proceedings of the ACM International Conference on Multimedia (ACM MM)*, 2019, pp. 2567–2575.
- [13] Yue Jing, Yujie Yang, Zongwei Liu, Yong Tian, and Nicu Sebe, “Hinet: Deep image hiding by invertible network,” in *Proceedings of the IEEE/CVF International Conference on Computer Vision (ICCV)*, 2021, pp. 4733–4742.
- [14] Sara Sabour, Nicholas Frosst, and Geoffrey E Hinton, “Dynamic routing between capsules,” *Advances in neural information processing systems*, vol. 30, 2017.
- [15] Ethan Perez, Florian Strub, Harm De Vries, Vincent Dumoulin, and Aaron Courville, “Film: Visual reasoning with a general conditioning layer,” in *Proceedings of the AAAI conference on artificial intelligence*, 2018, vol. 32.
- [16] Reza Shokri, Marco Stronati, Congzheng Song, and Vitaly Shmatikov, “Membership inference attacks against machine learning models,” in *2017 IEEE symposium on security and privacy (SP)*. IEEE, 2017, pp. 3–18.
- [17] Xavier Glorot and Yoshua Bengio, “Understanding the difficulty of training deep feedforward neural networks,” in *Proceedings of the 13th International Conference on Artificial Intelligence and Statistics (AISTATS)*, 2010, pp. 249–256.
- [18] Eirikur Agustsson and Radu Timofte, “Ntire 2017 challenge on single image super-resolution: Dataset and study,” in *IEEE Conference on Computer Vision and Pattern Recognition Workshops (CVPRW)*, 2017, Introduces the DIV2K dataset.
- [19] Tsung-Yi Lin, Michael Maire, Serge Belongie, James Hays, Pietro Perona, Deva Ramanan, Piotr Dollár, and C. Lawrence Zitnick, “Microsoft coco: Common objects in context,” in *European Conference on Computer Vision (ECCV)*. 2014, pp. 740–755, Springer.
- [20] Jia Deng, Wei Dong, Richard Socher, Li-Jia Li, Kai Li, and Li Fei-Fei, “Imagenet: A large-scale hierarchical image database,” in *IEEE Conference on Computer Vision and Pattern Recognition (CVPR)*, 2009, pp. 248–255.